JOURNAL OF OPTOELECTRONICS AND ADVANCED MATERIALS Vol. 9, No. 6, June 2007, p. 1852 - 1855

Simulation of second harmonic generation in InGaAs single quantum well laser diodes

V. A. POPESCU*, N. N. PUSCAS
Physics Department, University "Politehnica "of Bucharest,Splaiul Independentei 313, 060042 Bucharest, Romania

Using the finite element method, we analyze the modal phase matching between the mode at the fundamental frequency ω and the 3 rd order mode at the frequency 2ω in $In_{0.2}Ga_{0.8}As$/GaAs/AlGaAs graded index-separate confinement heterostructure-single quantum well waveguide laser. The waveguiding effect in the laser active region and a small number of modes ($TE_0(\omega)$, $TE_0(2\omega)$, $TE_1(2\omega)$ and $TE_2(2\omega)$) in the transversal direction explains the relatively strong emission of both the fundamental and second-harmonic waves.

(Received October 10, 2006; accepted April 26, 2007)

Keywords: Single quantum well waveguide laser diode, Quantum mechanics, Finite element method

1. Introduction

The numerical simulation of second harmonic generation in semiconductor lasers by using the modal phase matching is a very important issue for integrated optics and telecommunication applications [1-6].

The electric field of the laser radiation can act on the noncentrosymmetric optical semiconductors with a large susceptibility to produce a nonlinear polarization effect which to generate the second harmonic. However, satisfying the phase-matching condition is not straightforward in III-V semiconductors such as GaAs, because it is isotropic. The phase velocity mismatch can be compensated by waveguide dispersion (modal phase matching method) because the effective index decreases with increasing mode number, so one could match the effective indexes of the fundamental mode at ω to some higher order mode at 2ω. The overlap of the interacting fields can be enhanced by an optimization of the refractive index profile (geometry and material) of the waveguide [6-8]. A good spatial overlap between the mode profile at the fundamental wavelength λ and a higher order mode at the harmonic wavelength λ/2 was obtained for a M-shaped refractive index configuration [7-8]. For optical applications an output mode profile with a single lobe is advantageous (the even modes TE_2 or TE_4 show a single lobe in the laser active region). For a third-order-mode laser diode the fundamental order mode at λ/2 has a weaker overlap with the quantum well region, thus a weaker gain, in order to make the laser to operate into the phase matched mode [2].

In this paper the effective index for the fundamental mode and for second harmonic modes in an $In_{0.2}Ga_{0.8}As$/GaAs/ $Al_xGa_{1-x}As$ graded index-separate confinement heterostructure single quantum well waveguide are determined.

2. InGaAs single quantum well laser diode

The sample studied is an InGaAs/GaAs/AlGaAs waveguide laser diode where the active region is a separate confinement heterostructure with an 80 Å wide $In_{0.2}Ga_{0.8}As$ quantum well (Fig. 1). The quantum well was sandwiched between the GaAs spacer layers followed by AlGaAs graded index regions and cladding layers [5]. The distinctive feature of internal second harmonic generation radiation is the presence of several pairs of narrow peaks (λ = 0.467 μm and λ = 0.492 μm) symmetrically distributed on either side of the central second harmonic peak at 0.4795 μm, for an injection current of 500 mA. The pure second harmonic generation at 0.4795 μm is much less intense than some of the side peaks visible in the spectrum. The relatively strong emission of the internal second harmonic wave and the second harmonic "blue-green" radiations in InGaAs quantum well laser diodes indicates that this second order nonlinear optical process is enhanced by waveguiding in the laser active region [1].

The key factor for the enhancement of internal second harmonic generation is the design of the waveguide structure with material and geometry parameters such that the third order modes at 0.467 μm, 0.4795 μm, 0.492 μm have the same phase velocity as the fundamental mode at 959 μm. Also, the waveguide structure must be designed for maximum overlap between the third order $TE_2(2\omega)$ mode at the second-harmonic frequency and TE_0 (ω)and TM_0 (ω) modes at the fundamental frequency [3].

Reliable refractive index measurements on $In_xGa_{1-x}As$ and $Al_xGa_{1-x}As$ alloys are currently not available for a large number of the wavelengths λ and x-compositions. Using the Sellmeier equation for GaAs, the refractive

index of $In_xGa_{1-x}As$ alloys depends on the band gap energy e_g [9].

$$n(\lambda)=\sqrt{8.95+\frac{2.054}{1-(\frac{0.6245e_{g0}}{\lambda e_g})^2}},\ e_g=1.424-1.501+0.436x^2,\ e_{g0}=1.424 \tag{1}$$

The refractive index for each layer of the planar waveguide were found by a interpolation formula by using the band gap energy difference between the $Al_xGa_{1-x}As$ alloys and GaAs [9,10]

$$n(\lambda)=\sqrt{a_0(a_3+\frac{a_4}{2}(\frac{e_0}{d_0})^{1.5})+b_0}\ , \tag{2}$$

where:

$$a_0=6.3+19\,x,\ b_0=9.4-10.2\,x,$$
$$e_0=1.425+1.155\,x+0.37\,x^2,\ d_0=1.765+1.115\,x+0.37\,x^2,$$
$$a_1=\frac{hc}{\lambda e_0 e_v},\ a_2=\frac{hc}{\lambda d_0 e_v},\ a_3=\frac{2-\sqrt{1+a_1}-\sqrt{1-a_1}}{a_1^2},\ a_4=\frac{2-\sqrt{1+a_2}-\sqrt{1-a_2}}{a_2^2},$$
$$h=6.626\times10^{-34}\ \text{js},\ c=2.99792\times10^8\ \text{m/s},\ e_v=1.60217653\times10^{-19}\ \text{eV} \tag{3}$$

The dispersion relation shows that increasing aluminum concentration produce decreasing refractive indices and the bandgap of $Al_xGa_{1-x}As$ is slightly larger than that for GaAs according to the approximate relation of e_0.

We have solved the wave equations for the given boundary conditions (the Dirichlet boundary condition at the ends of the interval where the wave function can be approximated with 0 and the Neuman boundary condition for each coordinate of the interfaces) by using the Galerkin's variant of the finite element method, with triangular grid and variable step [11].

3. Numerical results and conclusions

The investigated device at the fundamental wavelength (λ = 0.959 μm) and at the second harmonic (λ = 0.4795 μm) consist in an InGaAs/GaAs/AlGaAs waveguide laser diode where the active region is a separate confinement heterostructure with an 80 Å wide $In_{0.2}Ga_{0.8}As$ quantum well (Figs. 1-2). The refractive indices at the fundamental (second-harmonic) wave of the cladding materials ($Al_{0.6}Ga_{0.4}As$), linearly graded-index region ($Al_{0.6}Ga_{0.4}As$-$Al_{0.05}Ga_{0.05}As$), spacer layers (GaAs) and quantum well ($In_{0.2}Ga_{0.8}As$) are n_1 = 3.20088 (3.29077), n_2 = 3.20088-3.50901 (3.29077-3.622442), n_3 = 3.53784 (3.72195), and n_4 = 3.87237 (4.36686), respectively. Due to the small thickness of the core region, the wave propagation is restricted to the fundamental mode in transversal direction. In this direction we have only four modes ($TE_0(\omega)$, $TE_0(2\omega)$, $TE_1(2\omega)$ and $TE_2(2\omega)$). Our calculated value of the effective propagation constant by using the finite element method for the fundamental mode TE_0 at the fundamental frequency ω and for the second-harmonic mode TE_2 at the frequency 2ω in waveguide laser is β/k = 3.3. Thus, the phase velocity mismatch between the mode at the fundamental frequency ω and the 3rd order mode (TE_2) at the frequency 2ω can be compensated by the waveguide dispersion and the modal phase matching condition is accomplished. The effective index of the third-order mode is close to the cladding index (Fig. 2). The exact value depends on the precise value of the refractive index and on the exact composition of the sample. Unfortunately, the refractive indices of AlGaAs alloy are known within a certain error.

The bandgap discontinuities of the quantum well, spacer layers and graded-index region confine the carries (electrons and holes) to the active core region, forcing them to occupy a planar region. Furthermore, the optical waveguide confines the light to regions of high gain. Fig. 3 shows the calculated electric field (normalized to a maximum value of 1) for the fundamental modes $TE_0(\omega)$, $TE_0(2\omega)$ and for $TE_2(2\omega)$ mode in single-quantum-well waveguide. While the fundamental spectra are quite broad, the second-harmonic signals are much narrower since they result from a nonlinear optical interaction involving only the dominant fundamental mode.

The calculated electric field for the $TE_2(2\omega)$ mode is similar with the experimental second harmonic component [12]. Fig. 4 shows a typical electric field for the fundamental mode (λ = 0.959 μm) and for the pairs of narrow peaks (λ = 0.467 μm and λ = 0.492 μm) symmetrically distributed on either side of the central second harmonic peak at λ = 0.4795 μm, for an injection current of 500 mA. Our simulation of the 2D optical waveguide (Fig. 5) shows a cross section of the electric field parallel (lateral) and perpendicular (depth) to the substrate surface for the fundamental mode $TE_0(\omega)$. Besides the fundamental mode we have a number of lateral modes.

The observed peaks of second harmonic and "blue-green" radiations are spectrally narrow [1]. Thus, the second-harmonic spectra of the "blue" radiation (λ = 0.467 μm) presents a full-width at half-maximum (FWHM) of about 1.6 nm and the corresponding fundamental wave had a spectral FWHM (Fig. 6) of about 3.07 nm (for an injection current I = 500 mA), and therefore only a fraction of the input badwidth is used in the conversion process [3].

The waveguiding effect in the laser active region and a small number of modes ($TE_0(\omega)$, $TE_0(2\omega)$, $TE_1(2\omega)$ and $TE_2(2\omega)$) in the transversal direction explains the relatively strong emission of both the fundamental and second-harmonic waves. Our numerical solution to the wave equation that describes the mode profile in a laser

structure can be used to optimize the design of a complicated waveguide structure with large discontinuities in the refractive index distribution.

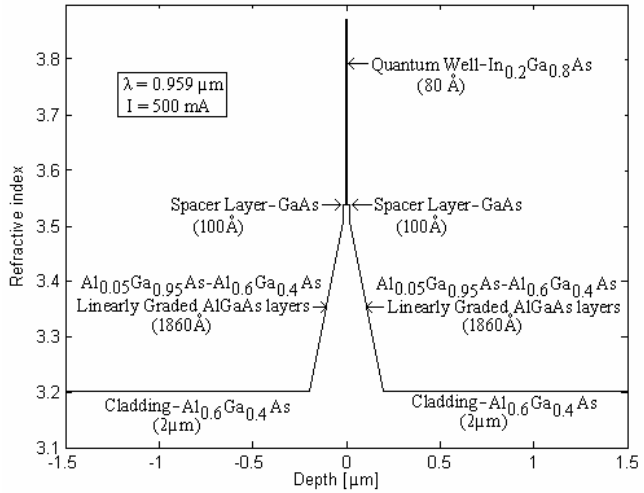

Fig. 1. Refractive index profile in $In_{0.2}Ga_{0.8}As/GaAs/AlGaAs$ graded index-separate confinement heterostructure - single quantum well waveguide.

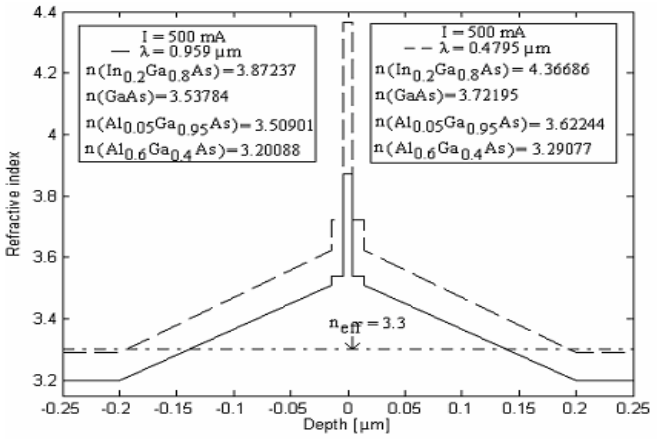

Fig. 2. Refractive index profile in $In_{0.2}Ga_{0.8}As/GaAs/AlGaAs$ graded index-separate confinement heterostructure-single quantum well waveguide for the fundamental wave at λ_{ω} = 0.959 μm (-) and for the harmonic wave at $\lambda_{2\omega}$ = 0.4795 μm (- -). The effective index n_{eff} (- . -) lies below the core index.

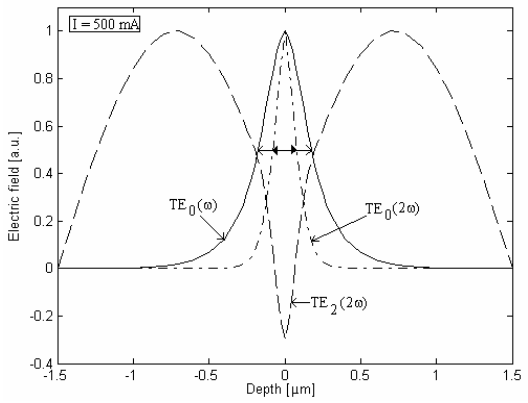

Fig. 3. The calculated electric field for the fundamental modes $TE_0(\omega)$, $TE_0(2\omega)$ and for $TE_2(2\omega)$ mode.

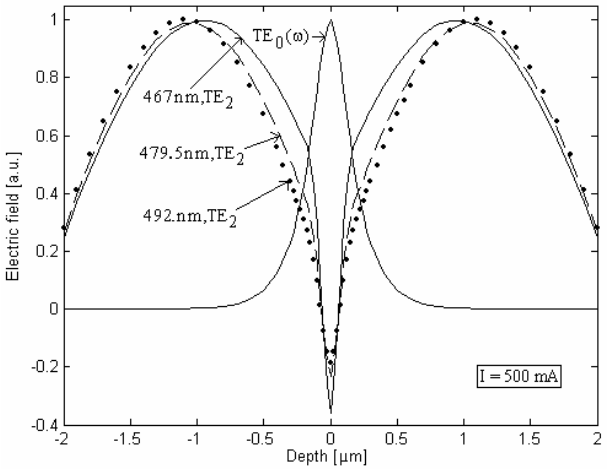

Fig. 4. The transversal electric field for the fundamental mode (λ = 0.959 μm) and for the pairs of narrow peaks (λ = 0.467 μm and λ = 0.492 μm) symmetrically distributed on either side of the central second harmonic peak at λ = 0.4795 μm, for an injection current of 500 mA.

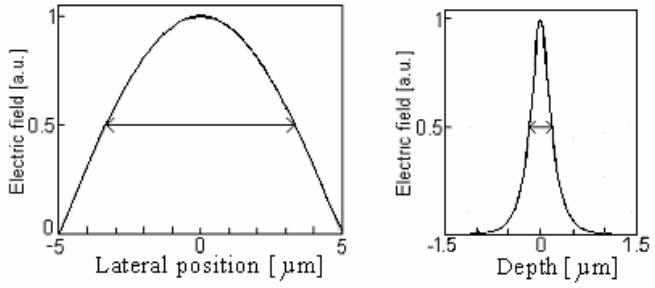

Fig. 5. Cross section of the electric field parallel (lateral) and perpendicular (depth) to the substrate surface for the fundamental mode $TE_0(\omega)$.

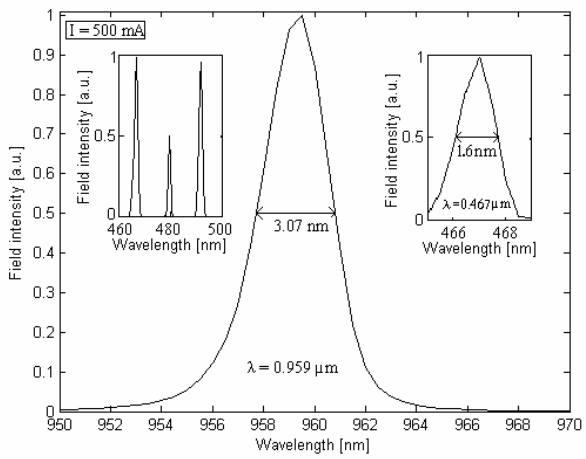

Fig. 6. The field intensity for the fundamental mode TE_0 (λ_ω = 0.959 μm) as a function of wavelength for an injection current I = 500 mA. The insets shows the field intensity spectrum for pure second harmonic generation ($\lambda_{2\omega}$ = 0.4795 μm) and for the pairs of side peaks (λ = 0.467 μm and λ = 0.492 μm).

References

[1] R. G. Ispasoiu, E. Smeu, N. N. Puscas, I. M. Popescu, G. I. Suruceanu, J. Mod. Optics. **47**, 1149 (2000).
[2] A. De Rossi, V. Ortiz, M. Calligaro, B. Vinter, J. Nagle, S. Ducci, V. Berger, Semicond. Sci. Technol. **19**, L99 (2004).
[3] K. Moutzouris, S. V. Rao, M. Ebrahimzadeh, A. De Rossi, M. Calligaro, V. Ortiz, V. Berger, Appl. Phys. Lett. **83**, 620 (2003).
[4] R. G. Ispasoiu, N. N. Puscas, I. M. Popescu, V. P. Yakovlev, E. Smeu, A. Toma, Int. J. Optoelectron. **11**, 127 (1997).
[5] N. Chand, S. N. G. Chu, N. K. Dutta, J. Lopata, M. Geva, A. V. Syrbu, A. Z. Mereutza, V. P. Yakovlev, IEEE J. of Quant. Electron. **30**, 424 (1994).
[6] L. J. Mawst, D. Botez, C. Zmudzinski, C. Tu, IEEE Photon. Technol. Lett. **11**, 1204 (1992).
[7] A. Chowdhury, L. McCaughan, IEEE Photon. Technol. Lett. **12**, 486 (2000).
[8] B. Oster, H. Fouckhardt, IEEE Photon. Technol. Lett. **13**, 672 (2001).
[9] BATOP optoelectronics, Semiconductor optoelectronic devices (2006).
[10] S. Adachi, J. Appl. Phys. **58**, R1 (1985).
[11] V. A. Popescu, Phys. Lett. A **297**, 338 (2002).
[12] A. Syrbu, A. Z. Mereutza, G. I. Suruceanu, V. P. Yakovlev, A. Caliman, A. T. Lupu, S. Vieru, M. Predescu, I. M. Popescu, R. G. Ispasoiu, Opt. Eng. **35**, 1278 (1996).

*Corresponding author: cripoco@physics.pub.ro